Phase States of Multiterminal Mesoscopic Normal-Metal–Superconductor Structures

P. Virtanen,[1] J. Zou,[2] I. Sosnin,[2,*] V. T. Petrashov,[2] and T. T. Heikkilä[1]

[1]*Low Temperature Laboratory, Helsinki University of Technology, P.O. Box 3500, FIN-02015 TKK, Finland*
[2]*Department of Physics, Royal Holloway, University of London, Egham, Surrey TW20 0EX, United Kingdom*

(Received 18 June 2007; published 21 November 2007)

We study a mesoscopic normal-metal structure with four superconducting contacts, two of which are joined into a loop. The structure undergoes transitions between three (meta)stable states, with different phase configurations triggered by nonequilibrium conditions. These transitions result in spectacular changes in the magnetoresistance. We find a qualitative agreement between the experiments and a theory based on the quasiclassical Keldysh formalism.

DOI: 10.1103/PhysRevLett.99.217003 PACS numbers: 74.45.+c, 72.15.Lh, 72.15.Qm

Conductance of a mesoscopic normal metal (N) with two contacts to superconductors (S) is an oscillating function of the phase difference ϕ of the order parameters in the contacts [1]. Such a system is called an Andreev interferometer as the oscillations are a result of quantum interference of quasiparticles that are Andreev reflected at the NS interfaces [2]. The influence of the phase on the observables of mesoscopic conductors [3–5] is reciprocated by the fact that the electronic properties of the N side affect the phase state of the superconductors. Examples of this are the π-states found in nonequilibrium S-N-S Andreev interferometers [6,7] and in S-F-S junctions [8,9], where F stands for a ferromagnet. A two-contact Andreev interferometer is characterized by a single phase difference ϕ whose value in equilibrium minimizes a free energy. Such phase states may be stable or metastable, as in interferometers with superconducting loops [10] in the presence of screening effects. In the general case of n S-N contacts the system should be described by a phase vector $\vec{\phi} = (\phi_1, \phi_2, \ldots, \phi_n)$ with components corresponding to phases ϕ_i of different superconductors. Up to date mesoscopic N-S systems with multiple superconducting contacts with the problem of stability of different phase configurations have not been addressed to our knowledge.

In this Letter we investigate experimentally and theoretically hybrid N-S structures [see Fig. 1(a)] consisting of a normal wire at the center, connected to a normal reservoir R on the right and a wide normal island L on the left. The center wire has four contacts to superconductors, and in some of the samples we also introduced thermometers Th_1 and Th_2, which did not essentially affect the results of measurements. Two of the contacts, S_1 and S_1', are joined into a loop, so that the superconducting phase difference between them is fixed by the magnetic flux. The total phase configuration of S_1, S_1', S_2, and S_3 is set through stability arguments. We used the magnetoresistance to probe the phase configuration, which is a technique used recently to measure the phase states of a flux qubit [5]. This does not require additional structures as needed, e.g., in flux measurements [9]. By applying control current I_H to the contacts H_1 and H_2 we were able to drive electrons into nonequilibrium. In the absence of the control current we observe the well-established flux periodic oscillations [1,3,4]. The oscillation pattern changes dramatically under nonequilibrium conditions (see Fig. 2), showing spectacular transitions between states with different phase configurations (Fig. 3). By studying the stable points of the phase dynamics, we identify the possible phase configurations as those shown in Fig. 1(c). The result can be understood as follows: First, the phases $\pm\phi/2$ on the S_1 contacts are fixed by the applied magnetic flux Φ_{loop}, and the phases

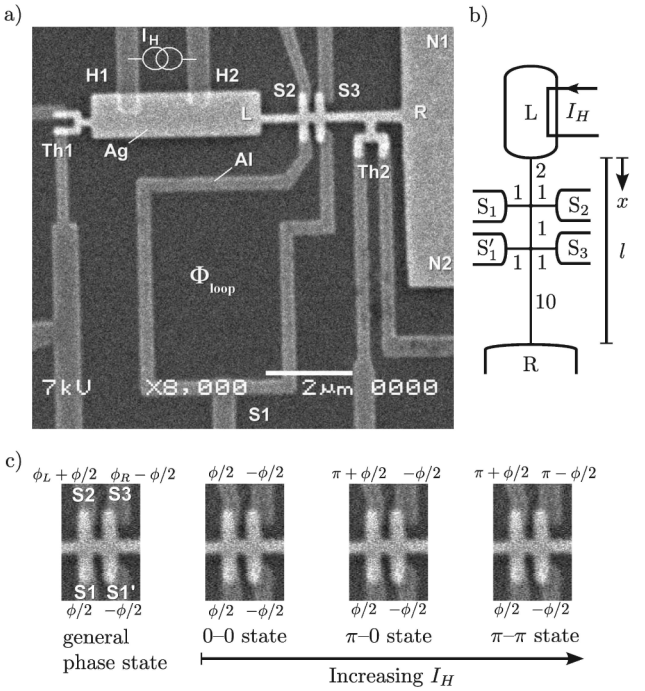

FIG. 1. (a) SEM micrograph of the measured sample. (b) Theoretical model, with the assumed relative lengths of the wires indicated. (c) Notation for the superconducting phases, and the three stationary phase states, in a region magnified from (a). Which one is stable depends on the value of I_H.

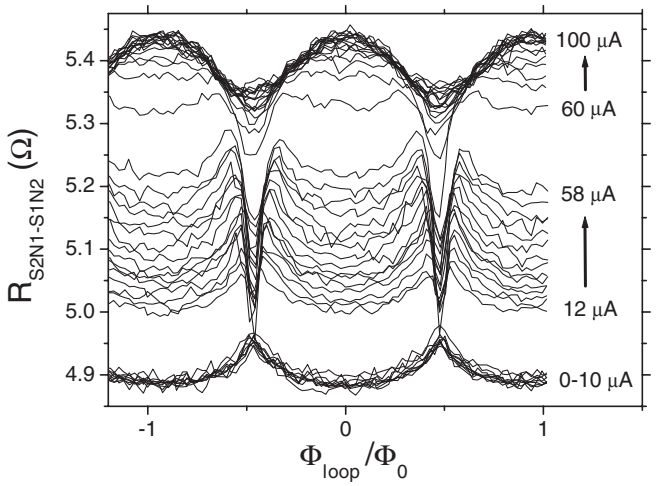

FIG. 2. Magnetoresistance oscillations at $T = 0.27$ K and at different currents I_H applied to leads H_1-H_2. Measuring current leads are S_2 and N_1; potential leads, S_1 and N_2. Here, $\Phi_0 = h/2e$ is the magnetic flux quantum.

$\phi_{L/R}$ at S_2, S_3 must satisfy the condition that no current flows into S_2 and S_3. Suppose now the S-N-S links S_1-S_2 and S_1-S_3 did not affect each other—the cross-coupling does not essentially change the conclusions (see below). Then, $I_{1-2}(\phi_L) = I_{1-3}(\phi_R) = 0$ would be achieved by $\phi_{L,R} = 0$ or π, as in usual S-N-S junctions, with the π-state realized only when the energy distribution of the electrons in the junction deviates sufficiently from its equilibrium form. [6,7] In our structure, a nonequilibrium generated in island L penetrates in the center wire, and is stronger at S_1-S_2 than at S_1-S_3. Increasing I_H should thus trigger consecutive switching of the two junctions, which then should be visible in the magnetoresistance.

The structures were fabricated using standard techniques (see, e.g., [1,5]). The normal part was made of

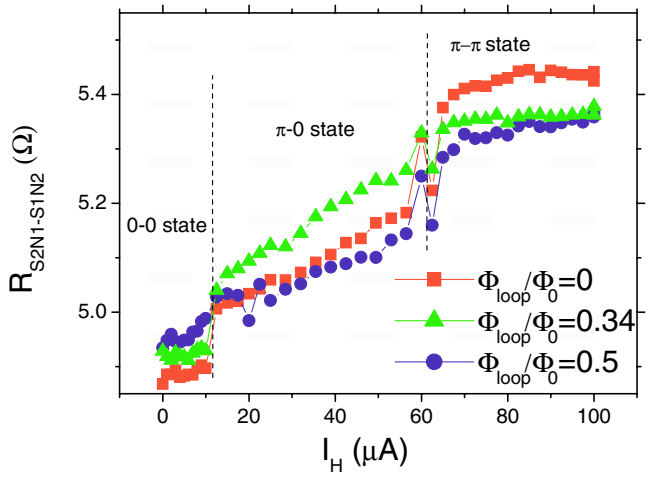

FIG. 3 (color online). Data from Fig. 2 presented as a function of I_H at different values of Φ_{loop}. We identify the different regions with the phase states in Fig. 1(c).

30 nm thick silver (Ag) film. The second layer was made of 55 nm thick aluminum (Al) film used as a superconductor. Resistivity of the Ag film was $\sim 2\ \mu\Omega$ cm with diffusion constants $D \sim 130$ cm^2/s. The right reservoir is in good thermal contact with massive Au pads so that its temperature is fixed by the substrate and the quasiparticle distribution function is close to its equilibrium form. The left island we call a quasireservoir, as the relaxation in it is insufficient to thermalize the electrons, but it is large enough to suppress the proximity effect from the central N-S contacts.

Figure 2 shows the magnetoresistance of the sample shown in Fig. 1 at various values of I_H. We see three distinct types of magnetoresistance oscillations: usual oscillations at $I_H < 12\ \mu$A changing according to the temperature variation created by I_H, oscillations with dips at $\Phi_{loop} = \frac{1}{2}\Phi_0$ for $12\ \mu\text{A} < I_H < 60\ \mu$A, and reversed oscillations at $I_H > 60\ \mu$A. These regions are illustrated in Fig. 3, which shows the resistance as a function of I_H for three values of the flux Φ_{loop}. When the sample is heated uniformly by changing the bath temperature T, the magnetoresistance remains qualitatively similar to the lowest curves in Fig. 2. This indicates that the jumps in the magnetoresistance occur due to nonequilibrium.

To describe the nonequilibrium transitions in our multiterminal structure, we model the dynamics of the phase vector $\vec{\phi}$. We assume that the superconducting terminals are in equilibrium, and employ a resistively and capacitively shunted Josephson junction model [11]

$$\frac{\hbar}{2e}\mathbf{C}\ddot{\vec{\phi}} = \vec{I}[\vec{\phi}] = \vec{I}^S(\vec{\phi}) + \frac{\hbar}{2e}\mathbf{G}[\vec{\phi}]\dot{\vec{\phi}}. \qquad (1)$$

The currents $\vec{I}$ entering the terminals drive the phases, which respond according to a capacitance matrix $\mathbf{C}$. Stability of stationary states, $\vec{\phi}(t) = \text{const}$, can be analyzed using standard methods for dynamical systems. It is useful to split the currents to a stationary part $\vec{I}^S(\vec{\phi})$ and a dissipative part, described by a conductance matrix $\mathbf{G}$. The former can be conveniently evaluated with the dirty-limit quasiclassical theory [12]. Finding the dissipative term within this theory is complicated [13], and we approximate $\mathbf{G}$ with a constant matrix. Conclusions below do not depend on the details of $\mathbf{C}$ and $\mathbf{G}$.

To model qualitatively the effect of nonequilibrium on $\vec{I}^S(\vec{\phi})$, we use the following approach. Assuming the inelastic scattering is sufficiently weak in quasireservoir L, the distribution function $f_q(E)$ there obtains a nonequilibrium form [14]. For simplicity, we neglect the effects of superconductivity on $f_q(E)$. In this case, the heating is described by the voltage $V_H \sim I_H$ across the heating contacts, resulting to the distribution function f_q,

$$2f_q(E) = f_0(E + eV_H/2 + \mu_{t,L}) + f_0(E - eV_H/2 + \mu_{t,L}). \qquad (2)$$

Reservoir R is assumed to be in equilibrium, and hence $f_R(E) = f_0(E + \mu_{t,R})$. Here $f_0(E) = [\exp(E/k_BT) + 1]^{-1}$ is the Fermi function at the lattice temperature T and $\mu_{t,L}$, $\mu_{t,R}$ are small thermoelectric potentials [15]. Using these boundary conditions in the Usadel equations [12,16,17], we have numerically evaluated the currents $\vec{I}^S(\vec{\phi}, V_H)$. To understand the results, it is useful to consider a slightly simplified analytical model. Neglecting proximity effect and concentrating on subgap $E < |\Delta|$ energies, the distribution function in the center wire is $f(E, x) = \frac{l-x}{l} f_q(E) + \frac{x}{l} f_R(E)$. The current entering terminal m then becomes [7,12]

$$I^S_{m,N}(\vec{\phi}) = \frac{\sigma A_m}{2e} \int_{-\infty}^{\infty} dE j^S_m(E, \vec{\phi})[1 - 2f(E, x_m)], \quad (3)$$

where j^S_m is the spectral supercurrent [16] entering terminal m and x_m the distance of the arm leading to the superconductor m from island L. The sign of $I^S_{m,N}$ can be changed and π-transitions induced by tuning f, [6,7] as illustrated in the inset of Fig. 4.

At equilibrium ($V_H = 0$), supercurrents can be written as a gradient of a potential, $\vec{I}^S(\vec{\phi}) = -\frac{e}{\hbar}\vec{\nabla}_{\vec{\phi}}\mathcal{F}(\vec{\phi})$. Then, the dynamics (1) tend to decrease the energy $\mathcal{E} = \frac{\hbar^2}{4e^2}\dot{\vec{\phi}} \cdot \mathbf{C}\dot{\vec{\phi}} + \mathcal{F}$, which implies that stable states occur at the minima of the "washboard" potential $\mathcal{F}$. However, in nonequilibrium in structures with $n > 2$ superconducting terminals, a nongradient component in $\vec{I}^S$ may feed energy to the phase dynamics. Here it arises due to the thermoelectric coupling. This is balanced by dissipation: analysis of Eq. (1) shows that a stationary state remains stable if $a \equiv \| \mathbf{H}_- \| \| \mathbf{H}_+^{-1} \|^{1/2} < (2\beta_c)^{-1/2}$, and $\mathbf{H}_+$ is positive (semi)definite. Here, $\beta_c \equiv 2eI_c \| \mathbf{R} \|^2 \| \mathbf{C} \| /\hbar$, $\mathbf{R}$ is the resistance matrix, $\mathbf{H}_\pm \equiv \frac{1}{2I_c}[\nabla_{\vec{\phi}}\vec{I}^S \pm (\nabla_{\vec{\phi}}\vec{I}^S)^\dagger]$ are the "curvature" and curl parts of the Jacobian, and $\| \cdot \|$ is the L^2 norm. Taking parameters $\| \mathbf{C} \| \sim 1$ fF, $\| \mathbf{R} \| \sim 10\ \Omega$, $I_c \sim 5\ \mu$A representative of our structure and using numerically calculated $\vec{I}^S$, we find $a \lesssim 1$ and $(2\beta_c)^{-1/2} \sim 18$, so that $\vec{I}^S$ can be approximated with a gradient field. For $a \gg (2\beta_c)^{-1/2}$, voltages $V = \hbar\dot{\phi}/2e$ could be induced between the superconductors.

To proceed analytically further, we can find the high-energy expansion for j_S in our multiterminal structure, [7,18] and evaluate Eq. (3). We then obtain the high-temperature limit for the potential

$$\mathcal{F}(\vec{\phi}) = \frac{\hbar^2}{4e^2}\frac{(\frac{2\pi\Phi_{loop}}{\Phi_0} - \phi)^2}{L} - \frac{\hbar}{2e}\sum_{mk}\left[\frac{x_m}{l} I_c^0(A_{mk}, d_{mk}, 0) + \frac{l - x_m}{l} I_c^0(A_{mk}, d_{mk}, V_H)\right]\cos(\phi_m - \phi_k),$$

$$I_c^0(A, d, V) \equiv \frac{-64\pi A\sigma}{3 + 2\sqrt{2}} \frac{k_BT}{e} \mathrm{Re}\frac{\partial}{\partial d} e^{-d\sqrt{(2\pi k_BT - ieV)/\hbar D}}, \quad (4)$$

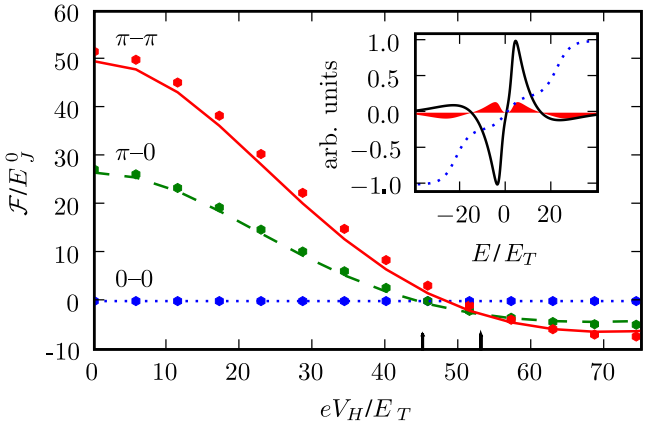

FIG. 4 (color online). Potential at the (approximate) stable phase states 0-0, π-0, and π-π as a function of the heating voltage V_H, for $\Phi = 0$, $L \to 0$, and $k_BT/E_T = 5$ in the geometry in Fig. 1(b). Numerical results are indicated by dots, Eq. (4) by lines. The potential is defined with respect to the state (0, 0) separately for each V_H, the Thouless energy $E_T \equiv \hbar D/d^2 \approx 50$ mKk_B corresponds to the distance d between S_2 and S_3, and $E_J^0 = \hbar E_T/(e^2 R_{S_2\text{-}S_3})$. The equilibrium state 0-0 is the ground state of the system for small V_H, and the transitions between the states occur at $V_H \sim 45E_T/e$ and $V_H \sim 53E_T/e$. These crossover voltages depend on Φ. They are also close to each other—the difference to the experiment is likely due to the simplified model for $f_q(I_H)$. Inset: Distribution function $1 - 2f$ (dotted line), the spectral supercurrent j_S (solid line), and their product (shaded) near S_1-S_3, for $V_H = 44E_T$. Large V_H increases the negative contribution to integral (3).

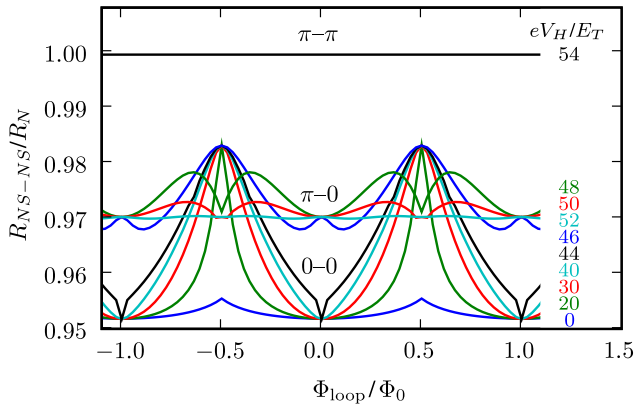

FIG. 5 (color online). Magnetoresistance for different heating voltages V_H calculated numerically (see text), normalized by the corresponding normal-state resistance R_N. Loop inductance $L \approx 150$ pH is assumed, and this reduces the oscillation amplitude in the regime $V_H/E_T \lesssim 20$. The theoretical linear-response N-S resistance does not depend on the choice of S terminals used for the measurement. For asymmetric structures, phase oscillations appear also in the π-π state.

where I_c^0 is the S-N-S supercurrent [7], L the inductance of the loop, d_{mk} the distance between terminals m and k along the wires, and A_{mk} an effective junction area. Assuming all the wires have the same cross section A, $A_{S_1S_2} = A_{S_1'S_3} = A/2$, and $A_{mk} = A/4$ for other pairings.

From Eq. (4), or the numerically integrated $\mathcal{F}$, it turns out that the possible stable states of the system correspond approximatively to the phase configurations shown in Fig. 1(c), for loop inductances $L \lesssim \hbar/2eI_c(V_H) \sim$ 300 pH (for the V_H at the first transition). For illustration, we plot in Fig. 4 the potential at these three states as a function of the heating voltage V_H. Some of the full potential data is shown in the auxiliary material [19].

We calculate the magnetoresistance by first finding the stable phase state within the approximations outlined above and then solving the conductance from the Usadel equations numerically, taking, e.g., nonlocal Josephson effects into account. [4,12] Results are illustrated in Fig. 5. The main qualitative features common to both theory and experiments are: (i) Noticeable change can be seen upon the change of the phase state. (ii) The resistances are lowest at the 0-0 state, intermediate for the π-0 state, and highest for the π-π state. (iii) In the 0-0 state, there is a resistance minimum for zero applied flux and a maximum when the flux is close to half a flux quantum. In the π-0 state, the resistance is at minimum for both of these values of the flux: an up-down symmetry of the structure would force the two resistances equal (for $L = 0$). In the theory, details of the oscillations depend on the geometrical symmetry of the structure. For the π-π state, the measured oscillations are inverted vs the 0-0 state. In the theoretical model, we have only found inverted oscillations for a small range of V_H close to the π-0 $\mapsto$ π-π crossover, but in principle there is no symmetry in the model that would forbid them for a wider range of V_H in a suitable geometry.

Our qualitative model (2) for the heating also requires a geometry different from the scanning electron microscopy (SEM) picture, see Fig. 1(b), to have a nonequilibrium sufficiently strong to produce two transitions. We attribute this to finite inelastic relaxation lengths and effects due to superconductivity in the heater. The latter also implies that comparing theoretical crossover voltages to the experiment is problematic. We also note that the measured N-S resistances $R_{S_1N_1-S_2N_2}$ and $R_{S_3N_1-S_2N_2}$ show only a single transition, whereas the theory predicts identical transitions for all resistances. This may be due to the measurement current $I_{\mathrm{meas}} \approx 0.2\ \mu$A, whose magnitude is comparable to the supercurrents, disturbing the phase configuration.

Summarizing, we have observed that the magnetoresistance of a multicontact Andreev interferometer shows transitions between different (meta)stable states. Theoretically, we explain these as different phase states, corresponding to separate nonequilibrium-induced 0-π transitions in two of the S-N-S Josephson junctions inside the interferometer. Our findings show how the conductance can be used to monitor the phase states, in accord with a recent suggestion [5].

We acknowledge the help from M. Meschke and J. P. Pekola. This work was supported by an EC-funded ULTI programme, from the EPSRC (Grant EP/E012469/1), the Academy of Finland and the Finnish Cultural Foundation.

*Deceased.

[1] V. T. Petrashov, V. N. Antonov, P. Delsing, and T. Claeson, Phys. Rev. Lett. **74**, 5268 (1995).
[2] A. F. Andreev, Sov. Phys. JETP **19**, 1228 (1964).
[3] C. J. Lambert and R. Raimondi, J. Phys. Condens. Matter **10**, 901 (1998); J. Eom, C.-J. Chien, and V. Chandrasekhar, Phys. Rev. Lett. **81**, 437 (1998); D. A. Dikin, S. Jung, and V. Chandrasekhar, Phys. Rev. B **65**, 012511 (2001).
[4] H. Courtois, *et al.*, J. Low Temp. Phys. **116**, 187 (1999); P. Virtanen and T. T. Heikkilä, Appl. Phys. A **89**, 625 (2007); V. K. Kaplunenko and V. V. Ryazanov, Phys. Lett. A **110**, 145 (1985); R. Shaikhaidarov, *et al.*, Phys. Rev. B **62**, R14 649 (2000).
[5] V. T. Petrashov, *et al.*, Phys. Rev. Lett. **95**, 147001 (2005).
[6] J. J. A. Baselmans, A. F. Morpurgo, B. J. van Wees, and T. M. Klapwijk, Nature (London), **397**, 43 (1999); A. F. Volkov, Phys. Rev. Lett. **74**, 4730 (1995).
[7] F. K. Wilhelm, G. Schön, and A. D. Zaikin, Phys. Rev. Lett. **81**, 1682 (1998).
[8] V. V. Ryazanov, *et al.*, Phys. Rev. Lett. **86**, 2427 (2001); A. I. Buzdin, L. N. Bulaevskiĭ, and S. V. Panyukov, JETP Lett. **35**, 178 (1982).
[9] S. M. Frolov, *et al.*, Phys. Rev. B **70**, 144505 (2004).
[10] V. T. Petrashov, R. S. Shaikhaidarov, and I. A. Sosnin, JETP Lett. **64**, 839 (1996).
[11] M. Tinkham, *Introduction to Superconductivity* (McGraw-Hill, New York, 1996), 2nd ed.
[12] W. Belzig, *et al.*, Superlattices Microstruct. **25**, 1251 (1999).
[13] J. C. Cuevas, *et al.*, Phys. Rev. B **73**, 184505 (2006).
[14] F. Giazotto, *et al.*, Rev. Mod. Phys. **78**, 217 (2006).
[15] R. Seviour and A. F. Volkov, Phys. Rev. B **62**, R6116 (2000); P. Virtanen and T. T. Heikkilä, Phys. Rev. Lett. **92**, 177004 (2004).
[16] T. T. Heikkilä, J. Särkkä, and F. K. Wilhelm, Phys. Rev. B **66**, 184513 (2002).
[17] K. D. Usadel, Phys. Rev. Lett. **25**, 507 (1970).
[18] P. Virtanen and T. T. Heikkilä, to be published.
[19] See EPAPS Document No. E-PRLTAO-99-067749 for supplementary materials. For more information on EPAPS, see http://www.aip.org/pubservs/epaps.html.